Supplementary Material

1 Model selection for vital rate functions

1.1 Survival function: $s(x)$

In the main text, we parameterized the survival function $s(x)$ using only individuals at 20 °C. As discussed in the main text, we chose to do this because individuals at this temperature were the only frogs that experienced mortality and we have substantial alternative evidence that the load-survival relationship between *R. muscosa* and *Bd* is not strongly temperature dependent. An alternative way that we could have parameterized the model was using all of the temperature data (4, 12, and 20 °C), but without including an effect of temperature. Given the link function $\text{logit}[s(x)] = b_0 + b_1 x$, the parameters change from $b_{0,\text{only 20 °C}} = 11.5973$ (SE: 4.74) to $b_{0,\text{all temperatures}} = 11.8241$ (SE; 4.16) and $b_{1,\text{only 20 °C}} = -0.8873$ (SE: 0.45) to $b_{1,\text{all temperatures}} = -0.8605$ (SE: 0.39) (Figure 1). Despite these seemingly small differences, our elasticity analysis shows that small changes in this survival function can have large effects on the ability of *R. muscosa* to persist through an epizootic.

1.2 Growth Function: $G(x', x)$

We explored a variety of different models for the growth functions $G(x', x)$ (Table 1, Figure 2). We did identify a more complex model than the model described in the manuscript that included a quadratic term for log zoospore size and an interaction between temperature and log zoospore load (Table 1; Model 6). We chose to use the linear model (Model 2) because 1) the quadratic model was highly specific for the data used to fit the model and did not give a generalizable *Bd* growth curve (e.g. exponential growth) and 2) for a given temperature the quadratic model did not allow for realistic extrapolation beyond the range of the data used to fit the model because for small log-zoospore loads the function predicts that increasing the log zoospore load at time t decreases log zoospore load at time $t + 1$ (i.e. when you are on the decreasing arm of the quadratic function, Figure 4). This is not a biologically reasonable pattern.

Despite these drawbacks, we ran the IPM analysis described in the paper using this quadratic growth model. We accounted for the zero derivative of the quadratic function by defining the growth function as the following piecewise function

$$G(x', x) \text{ if } \frac{d\mu(x,T)}{dx} > 0 \quad (1)$$

$$G(x', x_0) \text{ if } \frac{d\mu(x,T)}{dx} \leq 0 \quad (2)$$

where x_0 is the log zoospore load at which the derivate of $\mu(x,T) = b_0 + b_1 x + b_2 x^2 + b_3 T + b_4 xT$ is equal to 0. Analyzing the IPM with this growth function in place of the growth function used in the main text provided qualitatively similar results: population growth rate decreased with increasing temperature and the population growth rate was most sensitive to proportional changes in the parameters in the growth function $G(x', x)$ and the survival function $s(x)$. The major difference between the two growth functions is that the IPM model with the quadratic growth function predicted slower *Bd*-induced population declines than the linear model.

1.3 Loss of infection function: $l(x)$

The various models we fit for the loss of infection function $l(x)$ are given in Table 2. Model 3 and Model 5 are the best models based on AIC. Model 5 in which temperature is a factor has a marginally lower AIC than Model 3 in which temperature is continuous. A likelihood ratio test shows that Model 5 does not provide an overwhelmingly better fit than Model 3 ($\chi^2_{df=1} = 3.676$, $p = 0.055$) so we used the Model 3 (the linear model) because it allowed us to interpolate over all temperatures between 4 and 20 °C.

When fitting Model 3, there were three highly influential data points in which individuals lost infections after having a log zoospore of 8.3, 10.36, and 8.1. Individuals with these large losses had similar pre-loss loads at the next swabbing event (Figure 9), leading us to believe that these large losses were likely due to experimental error. Therefore, we excluded these points when fitting the model.

1.4 Initial infection burden function: $G_0(x')$

The various models we fit for the initial function burden function are given in Table 3. The normalized residuals of the full model were not significantly different than a normal distribution (Shapiro-Wilk test for normality: $p = 0.827$), thereby justifying the assumption of normality for the initial infection distribution. Similar to the loss of infection function, there were three outlying log-zoospore initial loads of 7.15, 8.26, and 11.81, which were the same spurious transitions observed in the loss of infection function, but in this case the points were an unrealistic gain in

zoospores after the unrealistic loss of zoospores (Figure 9). These points were again excluded from the analysis. After this exclusion, there was only one transition from 0 to infected at 20 °C. Diagnostic plots for the model used in the main text (given in bold in Table 3) are given in Figure 3.

1.5 Density-independent transmission function: $\phi(T)$

We explored three different density-independent transmission models. In the first model, the probability of infection was independent of temperature (Model 1). In the second model, temperature was a linear predictor of the probability of infection (Model 2). In the third model, temperature was a factor predicting the probability of infection. The model with a linear effect of temperature was the best model based on AIC criteria (Table 4).

2 The effect of eviction on the *Bd-Rana muscosa* Integral Projection Model

Given the parameterized density-independent IPM described in the main text, we examined the effects of eviction (loss of individuals from the model because their predicted future loads are outside the model range) using the examples and code given in Williams *et al.* (2012). In Table 5, we show the maximum size-dependent eviction value $\epsilon(x)$ as given by equation 2 in (Williams *et al.* 2012) for the host-parasite IPM model at four different temperatures. These values are non-zero, indicating that eviction is occurring in our parameterized IPM with a lower bound of -5 and an upper bound of 18. To assess the effect of eviction on the IPM predictions, we also show the value $d\lambda$ which gives the effect of eviction on the predicted population growth rate (Williams *et al.* 2012). For all temperatures between 4 and 20 °C (4 temperatures shown in Table 5), $d\lambda$ is very small indicating that despite eviction occurring in the parameterized IPM, it is having very little effect on the predictions of the IPM. Therefore, we felt confident in interpreting the IPM with the given upper and lower bounds.

3 R_0 for host-parasite Integral Projection Models

3.1 Derivation of R_0 for IPMs

Calculating R_0 for Integral Projection Models (IPM)s is challenging because IPMs can be used to represent the dynamics of both microparasites and macroparasites. Therefore, R_0 will need

to be computed and understood differently depending on the which type of parasite is being considered and the structure of the IPM. For microparasites, R_0 is defined as the average number of secondary infections produced by a typical infectious individual over its infective lifetime (Diekmann *et al.* 1990). For macroparasites, R_0 is defined as "the number of new female parasites produced by an average female parasite when there are no density-dependent constraints acting anywhere in the life cycle of the parasite" (Tompkins *et al.* 2002). We adopt a microparasite definition of R_0 for the remainder of this discussion, bearing in mind that a host-parasite IPM could easily be formulated such that the macroparasite definition of R_0 is more appropriate.

To define a microparasite R_0 for the host-parasite IPM described in the main text (equations 1 and 2), we start by considering density-dependent transmission such that the probability of becoming infected in a time step t is

$$\phi(I(x,t)) = 1 - \exp\left(\beta \int_L^U I(x,t)dx\right) \tag{3}$$

We then note that the host-parasite IPM model can be analogously stated as a (S)usceptible-(I)nfected-(S)usceptible model with a continuous $I(x)$ class. When analyzing the IPM model, it is standard practice to discretize the IPM into some number of n bins such that the IPM can be represented as a matrix model with a large number of classes (Coulson 2012). This could be thought of as re-expressing the SIS model with a continuous I class as an S-I_1-I_2-I_3-...-I_n-S model with many discrete I classes. Using this discretized approach, R_0 can be calculated using the methods described in Allen & van den Driessche (2008) and Klepac & Caswell (2011). Following the notation of Klepac & Caswell (2011), the partial matrix representation of the IPM that we use to calculate R_0 is given by

$$\begin{bmatrix} S \\ \mathbf{I} \end{bmatrix}(t+1) = \begin{bmatrix} 0 & 0 \\ M(\mathbf{I}) & N(\mathbf{I}) \end{bmatrix} \begin{bmatrix} S \\ \mathbf{I} \end{bmatrix}(t) = m(\mathbf{I}(\mathbf{t}))S(t) + \mathbf{U}\mathbf{I}(\mathbf{t}) = \mathbf{I}(t+1) \tag{4}$$

where the top two entries are 0 because they are not needed when calculating R_0 (i.e. R_0 only depends upon individuals entering the infected classes or individuals that are already in the infected classes), not because they are actually 0 in the IPM model (Oli *et al.* 2006; Klepac & Caswell 2011). $\mathbf{I}$ is a vector of length n that gives the various infected parasite load classes. $m(\mathbf{I})$ is a vector of length n where each element gives the probability of transitioning from class S (uninfected/susceptible) to an infected class with parasite load x_i where i is between 1 and n. We use this notation loosely as it is really the probability of transitioning to an infected class with a load in the interval $x_i \pm \Delta/2$ where x_i is the midpoint of this interval. Δ arises from

using the midpoint rule to evaluate the IPM (Easterling *et al.* 2000). Each ith element of the vector $m(\mathbf{I})$ is given by

$$m_i(\mathbf{I}(t)) = s_0\phi(\mathbf{I}(t))G_0(x_i)\Delta \tag{5}$$

where s_0 represents the probability of an uninfected individual surviving and $G_0(x_i)$ is the probability density function of transitioning from uninfected (S) to infected with a load of x_i as defined in the main text. Δ is needed to convert the probability density $G_0(x_i)$ to a probability.

$\mathbf{U}$ is a n x n matrix that specifies the transition probabilities of infected individuals among different load classes. The element in the ith row and the jth column of the matrix is given by

$$u_{ij} = s(x_j)(1 - l(x_j))G(x_i, x_j)\Delta \tag{6}$$

which gives the probability of an individual in the jth load class surviving ($s(x_j)$), not losing its infection ($1 - l(x_j)$), and transitioning to the load class of x_i in a time step ($G(x_i, x_j)$).

To calculate R_0, we then linearize $\mathbf{I}(t + 1)$ about a vector $\mathbf{n}^*$ which we set to be a host population with only susceptibles (Rohani *et al.* 2009; Klepac & Caswell 2011), $N^* = [S^* \; \mathbf{0}]$ where $\mathbf{0}$ is a vector of zeros of length n. We then compute the Jacobian matrix evaluated at $\mathbf{n}^*$

$$\mathbf{J} = \left.\frac{d\mathbf{I}(t+1)}{d\mathbf{I}(t)}\right|_{\mathbf{n}^*} \tag{7}$$

which allows us to compute R_0 (Klepac & Caswell 2011).

In the above case, one could compute $\mathbf{J}$ as follows. First compute, $\left.\frac{d\mathbf{U}\mathbf{I}(t)}{d\mathbf{I}(t)}\right|_{\mathbf{n}^*}$ which is simply $\mathbf{U}$. This is just the transition matrix for the infected individuals of various load classes. Next, compute $\left.\frac{dm(\mathbf{I}(t))}{d\mathbf{I}(t)}\right|_{\mathbf{n}^*}$, which results in a column vector $\mathbf{m}$ of length n where each element is given by

$$\frac{dm_i(\mathbf{I}(t))}{d\mathbf{I}(t)} = \beta s_0 S^* G_0(x_i)\Delta \tag{8}$$

Now let $\mathbf{M}$ be an n by n matrix with each column being equal to $\mathbf{m}$ so that $\mathbf{J} = \mathbf{M} + \mathbf{U}$. R_0 is then given by

$$R_0 = \max \text{ eig}(\mathbf{M}(\mathbb{1} - \mathbf{U})^{-1}) \tag{9}$$

where $\mathbb{1}$ is the identity matrix and $\mathbf{M}$ is equivalent to the "fertility" matrix described in Klepac & Caswell (2011). "max eig" refers to the maximum eigenvalue of this matrix.

A helpful approximation of this result can be derived by "collapsing" the various infected classes $\mathbf{I}(t)$ into a single infected class $I(t)$. The model is then reduced to a simple SIS model with the following transition matrix (where we again include 0s where the transitions do not affect the calculation of R_0)

$$\begin{bmatrix} S \\ I \end{bmatrix}(t+1) = \begin{bmatrix} 0 & 0 \\ s_0\phi(I(t)) & \bar{s}_I(1-\bar{l}) \end{bmatrix} \begin{bmatrix} S \\ I \end{bmatrix}(t) = s_0\phi(I(t))S(t) + \bar{s}_I(1-\bar{l})I(t) = I(t+1) \quad (10)$$

where $\bar{s}_I$ is the survival probability for an average infected individual and $\bar{l}$ is the probability of an average infected individual losing an infection.

Using the sames steps as above the resulting value of R_0 is

$$R_0 = \frac{\beta s_0 S^*}{1 - \bar{s}_I(1-\bar{l})} \quad (11)$$

3.2 Application of R_0 to *Bd-R. muscosa*

Using equations 9 and 11, we computed R_0 for the *Bd-Rana muscosa* system described in the main text as an illustrative example. Note that in this example, we assumed density dependent transmission without any probability of acquiring an infection from the environmental reservoir as we do in the main text. We make this simplification here because without accounting for the decay of the pathogen in the environment, an R_0 that accounts for both transmission due to the environment and other infected individuals would be trivially ∞ (Rohani *et al.* 2009). An environmental reservoir could be more explicitly incorporated in the host-parasite IPM by including an additional state variable $Z(t)$ which gives the total number of parasites in the environment at time t.

We set the transmission coefficient $\beta = 9.82e10^{-4}$ which was the transmission coefficient estimated in Rachowicz & Briggs (2007) for density-dependent transmission in *Bd-Rana muscosa* and assumed an initial susceptible population of 100 frogs ($S^* = 100$). Otherwise, all values for the hosts-parasite IPM were as given in Table 1 the main text. To compute $\bar{s}_I$ and $\bar{l}$ in equation 11, we assumed a density-independent host-parasite IPM (equations 7 and 8 in the main text) with $\phi = 1 - \exp(-\beta)$ and calculated the stable parasite load distribution conditional on infection ($p(x)$) giving the probability density of having some parasite load x. We used this probability distribution to compute the expected survival and loss probability of an average infected individual as $\bar{s}_I = \int_L^U s(x)p(x)dx$ and $\bar{l} = \int_L^U l(x)p(x)dx$, respectively.

Figure 10 shows the temperature dependence of R_0 for this illustrative example parameterized from the *Bd-R. muscosa* IPM. Notice that the approximation given by equation 11 is nearly identical to the predictions for R_0 from equation 9. At low temperatures, R_0 is less than 1 and proceeds to increase as temperature increases. At approximately 12 °C, R_0 ¿ 1. However, around 17 °C the R_0 reaches a maximum and begins to decline. This is due to the average probability of losing an infection $\bar{l}$ quickly and non-linearly decreasing as temperature increases and the average probability of surviving with an infection $\bar{s}_I$ holding relatively constant with temperature and then rapidly decreasing as temperature increases past 17 °C.

References

Allen, L.J. & van den Driessche, P. (2008) The basic reproduction number in some discrete-time epidemic models. *Journal of Difference Equations and Applications*, **14**, 1127–1147.

Coulson, T. (2012) Integral projections models, their construction and use in posing hypotheses in ecology. *Oikos*, **121**, 1337–1350.

Diekmann, O., Heesterbeek, J.A.P. & Metz, J.A.J. (1990) On the definition and the computation of the basic reproduction ratio R0 in models for infectious diseases in heterogeneous populations. *Journal of Mathematical Biology*, **28**, 365–382.

Easterling, M.R., Ellner, S.P. & Dixon, P.M. (2000) Size-specific sensitivity: applying a new structured population model. *Ecology*, **81**, 694–708.

Klepac, P. & Caswell, H. (2011) The stage-structured epidemic: Linking disease and demography with a multi-state matrix approach model. *Theoretical Ecology*, **4**, 301–319.

Oli, M.K., Venkataraman, M., Klein, P.A., Wendland, L.D. & Brown, M.B. (2006) Population dynamics of infectious diseases: A discrete time model. *Ecological Modelling*, **198**, 183–194.

Rachowicz, L.J. & Briggs, C.J. (2007) Quantifying the disease transmission function: effects of density on Batrachochytrium dendrobatidis transmission in the mountain yellow-legged frog Rana muscosa. *The Journal of Animal Ecology*, **76**, 711–21.

Rohani, P., Breban, R., Stallknecht, D.E. & Drake, J.M. (2009) Environmental transmission of low pathogenicity avian influenza viruses and its implications for pathogen invasion. *Proceedings of the National Academy of Sciences of the United States of America*, **106**, 10365–10369.

Tompkins, D.M., Dobson, A.P., Arneberg, P., Begon, M., Cattadori, I.M., Greenman, J.V., Heesterbeek, J.A.P., Hudson, P.J., Newborn, D., Pugliese, A., Rizzoli, A.P., Rosa, R., Rosso, F. & Wilson, K. (2002) Parasites and host population dynamics. P.J. Hudson, A. Rizzoli, B.T. Grenfell, H. Heessterbeck & A.P. Dobson, eds., *The Ecology of Wildlife Diseases*, chapter 3, pp. 45–62. Oxford University Press, Oxford.

Vredenburg, V.T., Knapp, R.A., Tunstall, T.S. & Briggs, C.J. (2010) Dynamics of an emerging disease drive large-scale amphibian population extinctions. *Proceedings of the National Academy of Sciences of the United States of America*, **107**, 9689–94.

Williams, J.T., Miller, T.E.X. & Ellner, S.P. (2012) Avoiding unintentional eviction from integral projection models. *Ecology*, **93**, 2008–2014.

Table 1: Candidate models for the growth function $G(x', x)$. All models assumed a normal distribution for the response variable. T is temperature, x is log zoospore size at time t, and r_i represents a random effect of an individual frog. The model with the bold AIC value is the model used in the main text.

Model	**Mean Component**	**Variance Component**	**AIC**
1	$\mu(x,T) = b_0 + b_1 x + b_2 T$	σ^2	1067.8
2	$\mu(x,T) = b_0 + b_1 x + b_2 T$	$\sigma^2(x) = \nu \exp(2cx)$	**1060.0**
3	$\mu(x,T) = b_0 + b_1 x + b_2 T$	$\sigma^2(x,T) = \nu \exp(2c_1 x + 2c_2 T)$	1060.7
4	$\mu(x,T)_i = b_0 + b_1 x + b_2 T + r_i$	$\sigma^2(x) = \nu \exp(2cx)$	1061.8
5	$\mu(x,T) = b_0 + b_1 x + b_2 T + b_3 xT$	$\sigma^2(x) = \nu \exp(2cx)$	1061.0
6	$\mu(x,T) = b_0 + b_1 x + b_2 T + b_3 xT + b_4 x^2$	$\sigma^2(x) = \nu \exp(2cx)$	1045.3
7	$\mu(x,T) = b_0 + b_1 x + b_2 T + b_3 x^2$	$\sigma^2(x) = \nu \exp(2cx)$	1049.3

Table 2: Candidate models for the loss of infection function $l(x)$. All models assumed a binomial distribution for the response variable. T is temperature, T_i is temperature as a factor, and x is log zoospore load at time t. The model with the bold AIC value is the model used in the main text.

Model	**Mean Component**	**AIC**
1	$\text{logit}(l(x)) = b_0 + b_1 x$	193.0
2	$\text{logit}(l(T)) = b_0 + b_1 T$	202.1
3	$\text{logit}(l(x,T)) = b_0 + b_1 x + b_2 T$	**180.4**
4	$\text{logit}(l(x,T)) = b_0 + b_1 x + b_2 T + b_3 xT$	182.4
5	$\text{logit}(l(x,T))_i = b_0 + b_1 x + T_i$	178.7

Table 3: Candidate models for the initial infection burden function $G_0(x')$. All models assumed a normal distribution for the response variable. T is temperature, T_i is temperature as a factor, and x is log zoospore load at time t. The model with the bold AIC value is the model used in the main text.

Model	**Mean Component**	**Variance Component**	**AIC**
1	$\mu(T) = b_0 + b_1 T$	σ^2	149.2
2	$\mu(T)_i = b_0 + T_i$	σ^2	148.5
3	$\mu(T) = b_0 + b_1 T$	$\sigma^2(T) = \nu \exp(2cT)$	**145.2**

Table 4: Candidate models for the density-independent transmission function $\phi(T)$. All models assumed a binomial distribution for the response variable. T is temperature and T_i is temperature as a factor. The model with the bold AIC value is the model used in the main text.

Model	**Mean Component**	**AIC**
1	$\text{logit}(\phi) = b_0$	198.0
2	$\text{logit}(\phi(T)) = b_0 + b_1 T$	**193.9**
3	$\text{logit}(\phi(T)_i) = b_0 + T_i$	195.8

Table 5: Table shows the effect of eviction on the *Batrachocytrium dendrobatidis-Rana muscosa* Integral Projection Model described in the main text at 4 different temperatures. $\epsilon(x)$ specifies the maximum value of eviction occurring in the IPM model as given by equation 2 in Williams *et al.* (2012). A value of zero indicates no eviction is occurring while a non-zero value indicates that eviction is occurring in the IPM. $d\lambda$ gives the effect of this eviction on the predicted population growth rate. In other words, how much would this growth rate change if no eviction was occurring. Despite eviction occurring in the *Bd-R. muscosa* IPM, it is having little effect on the predicted population growth rate.

***Bd-R. muscosa* IPM**	$\epsilon(x)$	$d\lambda$
at 4 °C	0.32	2.26e-05
at 10 °C	0.26	2.74e-05
at 15 °C	0.22	2.52e-05
at 20 °C	0.18	1.45e-08

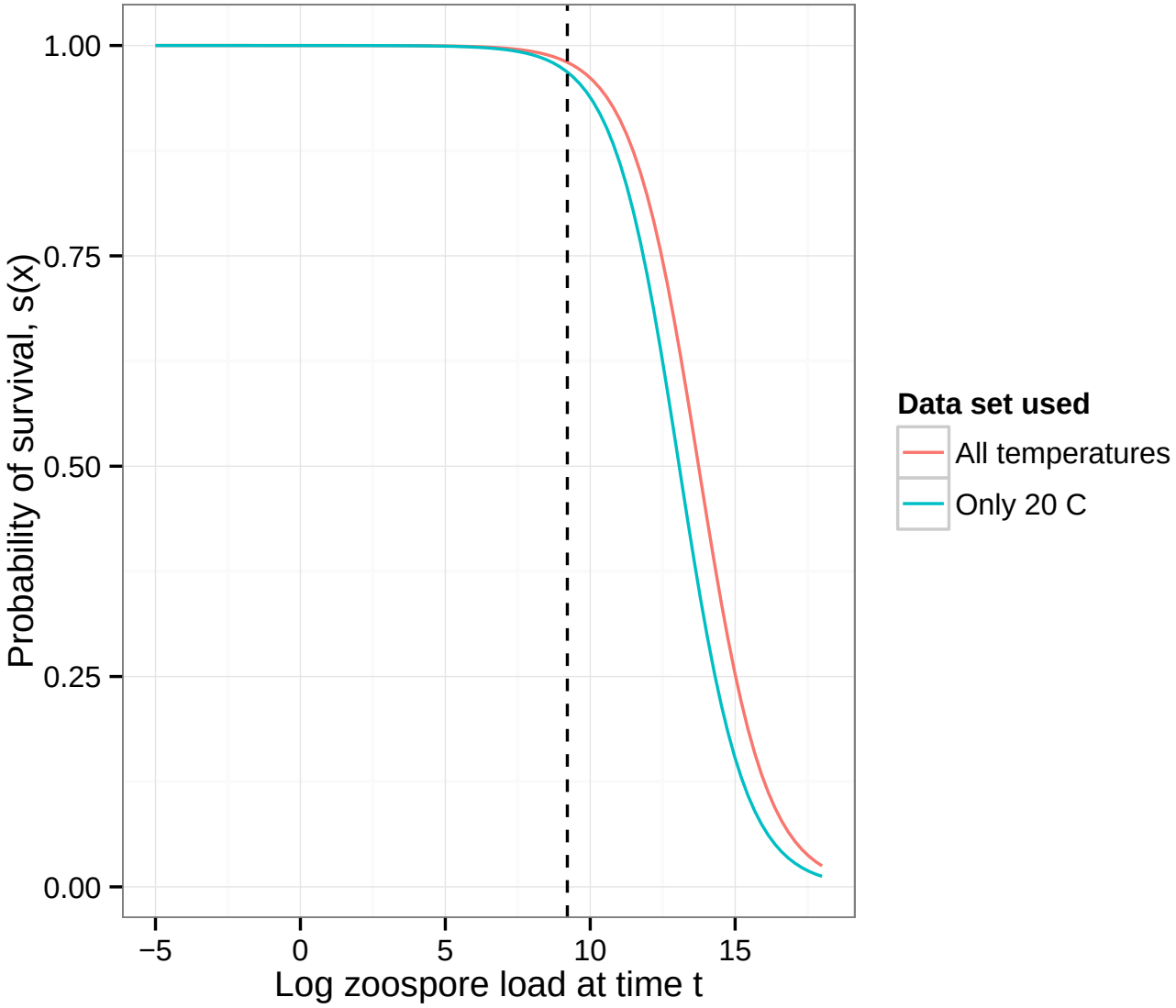

Figure 1: Comparison of survival functions fit from two different subsets of the data. The blue line shows the survival function used in the Integral Projection Model (IPM) analysis described in the main text and only includes data from individuals housed at 20 °C. The red line shows an alternative survival function that was parameterized using the data from all temperatures used in the experiment (4, 12, 20 °C). The dashed vertical line gives the 10,000 zoospore threshold reported by Vredenburg *et al.* (2010), which gives an approximate threshold at which *R. muscosa* begins to experience *Bd*-induced mortality in the field. While the survival curves from the two models are very similar, our elasticity analysis shows that even this small difference can have large effects on whether an *R. muscosa* population can persist through an epizootic at high temperatures.

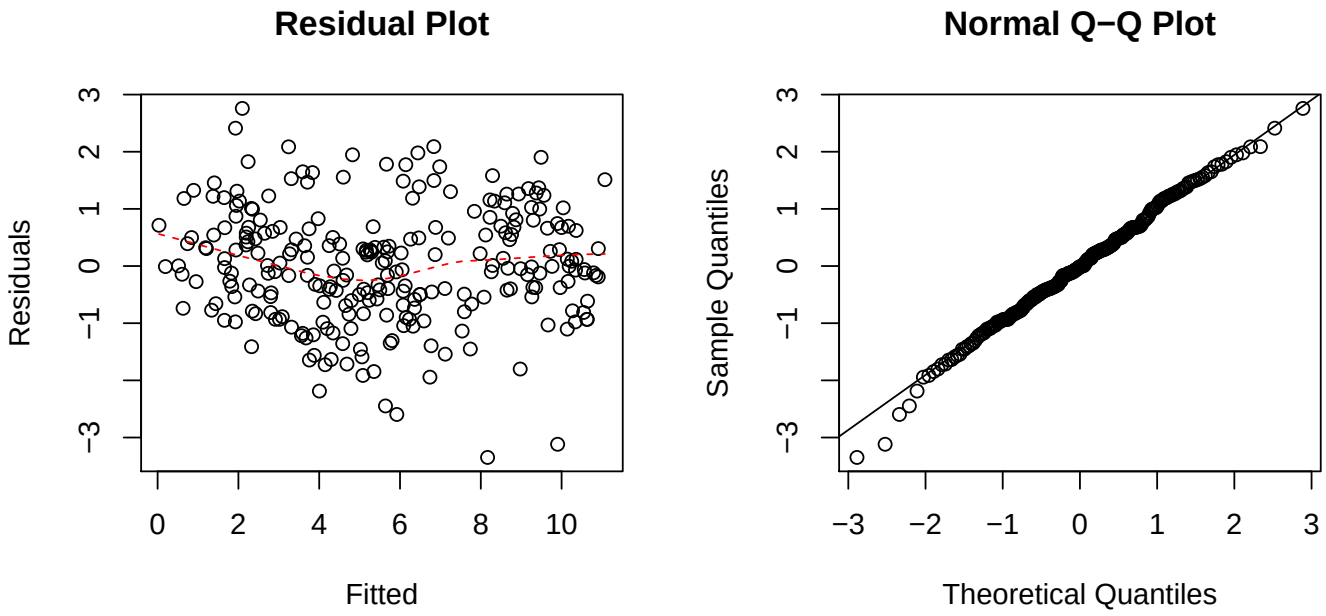

Figure 2: Diagnostic plots for the Model 2 in Table 1. The noticeable pattern in the residual plot (red line) can be accounted for with a quadratic term in the growth function (Model 6, Table 1). As discussed in the subsection *Growth Function:* $G(x', x)$ we chose to use this linear model for the growth function, but explored the effects of the alternative, non-linear growth function on the IPM predictions.

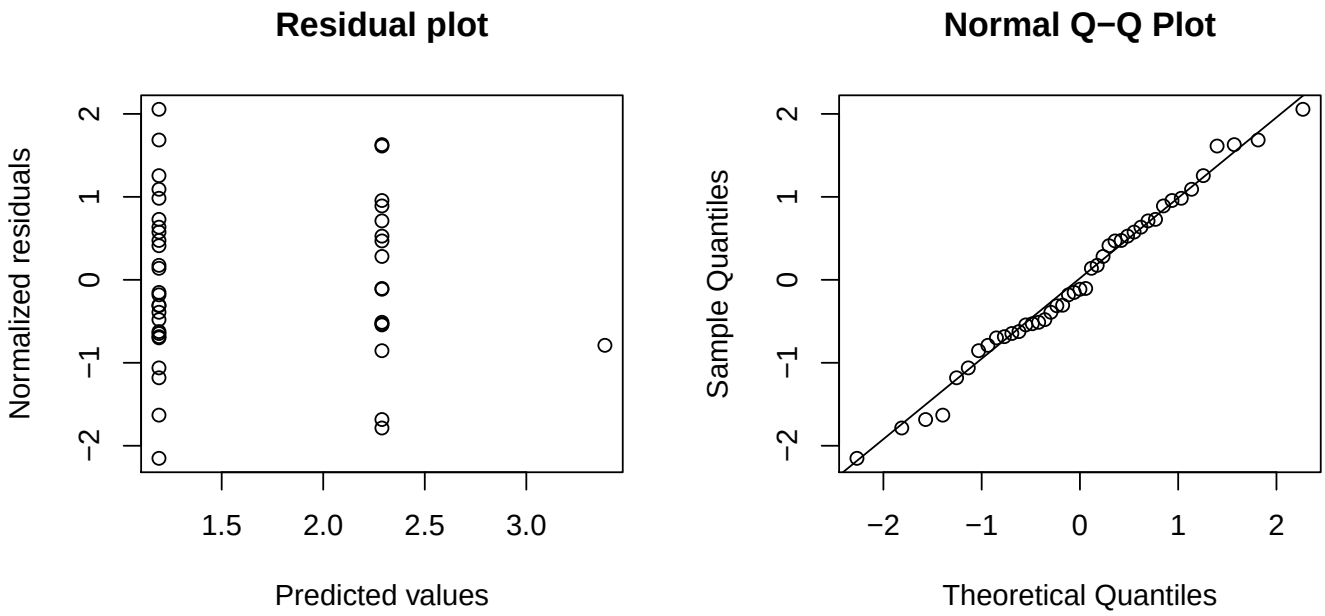

Figure 3: Diagnostic plots for the Model 3 in Table 3. The data point to the far right in the residual plot shows the single data point for a transition of an individual from 0 to infected at a temperature of 20 °C.

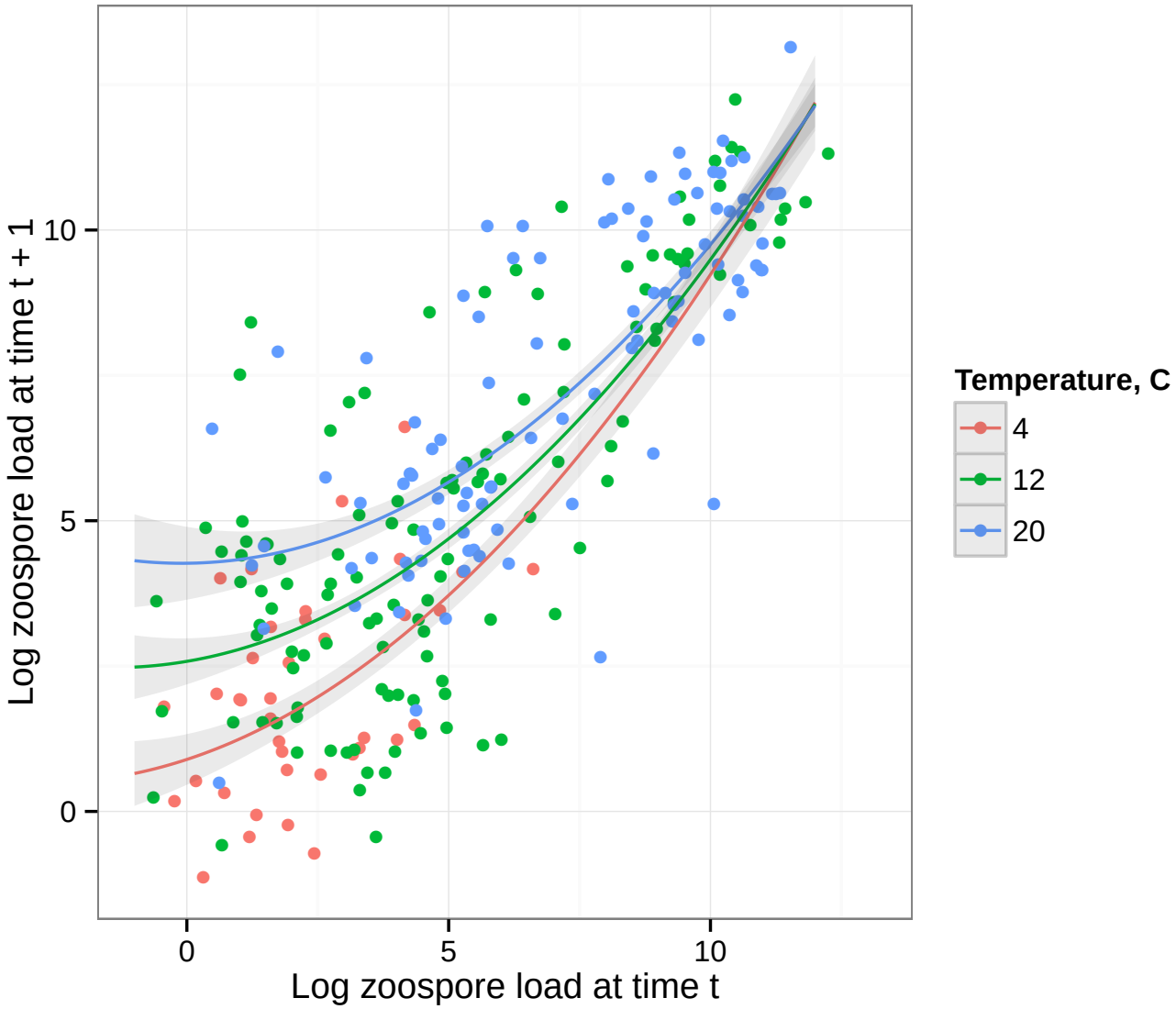

Figure 4: The best fit quadratic empirical growth function given by Model 6 in Table 1. As log-zoospore load at time t decreases the growth function flattens and eventually begins to increase for small enough values of log-zoospore load at time t.

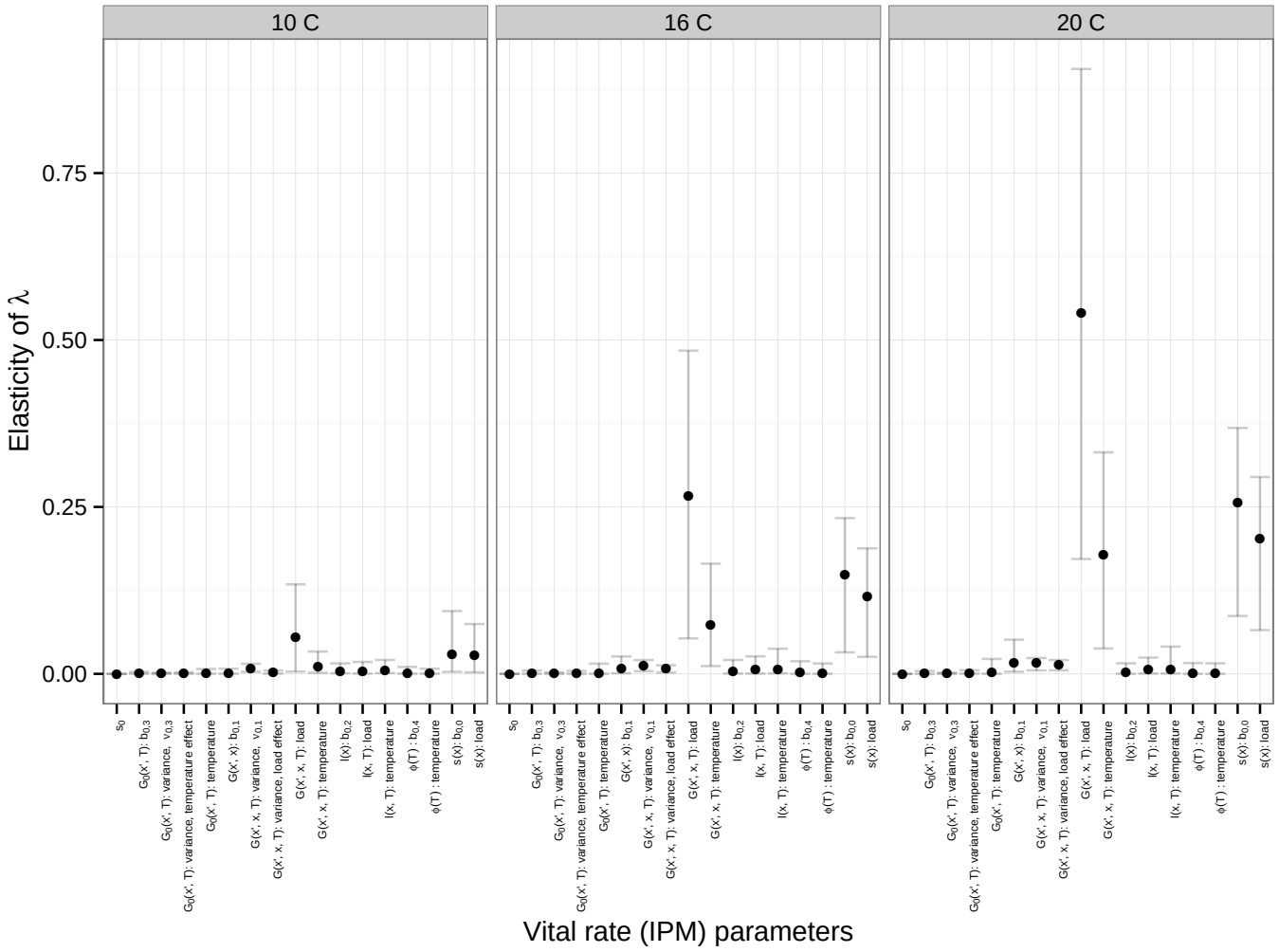

Figure 5: A local elasticity analysis of the population growth rate λ to the vital rate parameters used in the *Bd-Rana muscosa* IPM. The x axis gives all the vital rate parameters used in the *Bd-R. muscosa* IPM model. Each x axis label specifies the vital rate function to which a parameter belongs as well as the identity of that parameter. The parameters labeled as $b_{0,j}$ represent the intercepts of the given vital rate functions. The parameters labeled as load and temperature identify the load and temperature parameters of the given vital rate function. The parameters specified as variance refer to the parameters affecting the variance of the vital rate function, where $\nu_{0,j}$ gives the variance of the vital rate function when the effect of other covariates on the variance is 0. The points represent the median elasticity of λ to a given parameter based on 1000 simulations and the error bars give the first and third quartiles of the uncertainty around this elasticity.

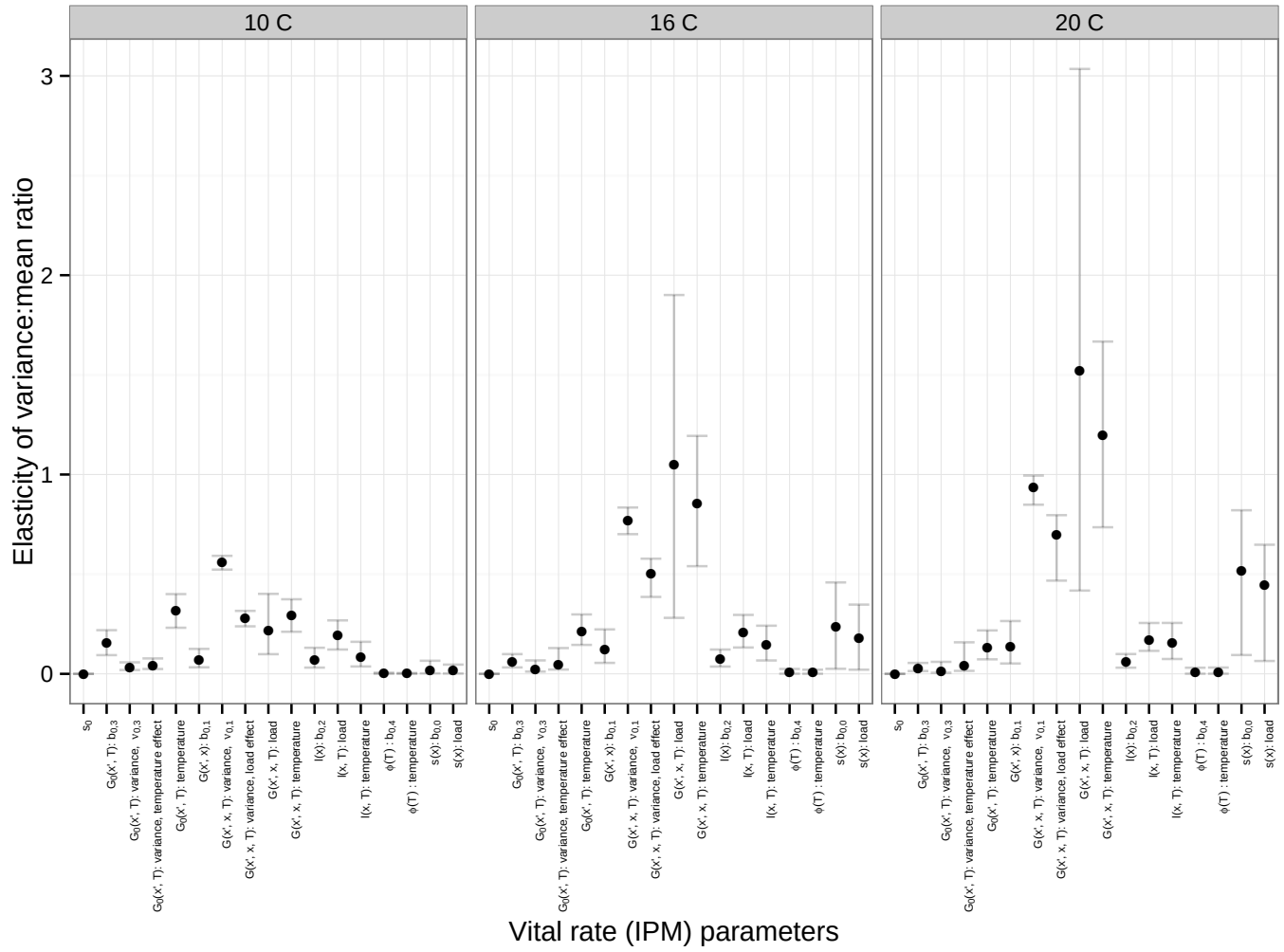

Figure 6: A local elasticity analysis of the variance to mean ratio of the *Bd* load distribution to the vital rate parameters used in the *Bd-Rana muscosa* IPM. The x axis gives all the vital rate parameters used in the *Bd-R. muscosa* IPM model. Each x axis label specifies the vital rate function to which a parameter belongs as well as the identity of that parameter. The parameters labeled as $b_{0,j}$ represent the intercepts of the given vital rate functions. The parameters labeled as load and temperature identify the load and temperature parameters of the given vital rate function. The parameters specified as variance refer to the parameters affecting the variance of the vital rate function, where $\nu_{0,j}$ gives the variance of the vital rate function when the effect of other covariates on the variance is 0. The points represent the median elasticity of the variance to mean ratio to a given parameter based on 1000 simulations and the error bars give the first and third quartiles of the uncertainty around this elasticity.

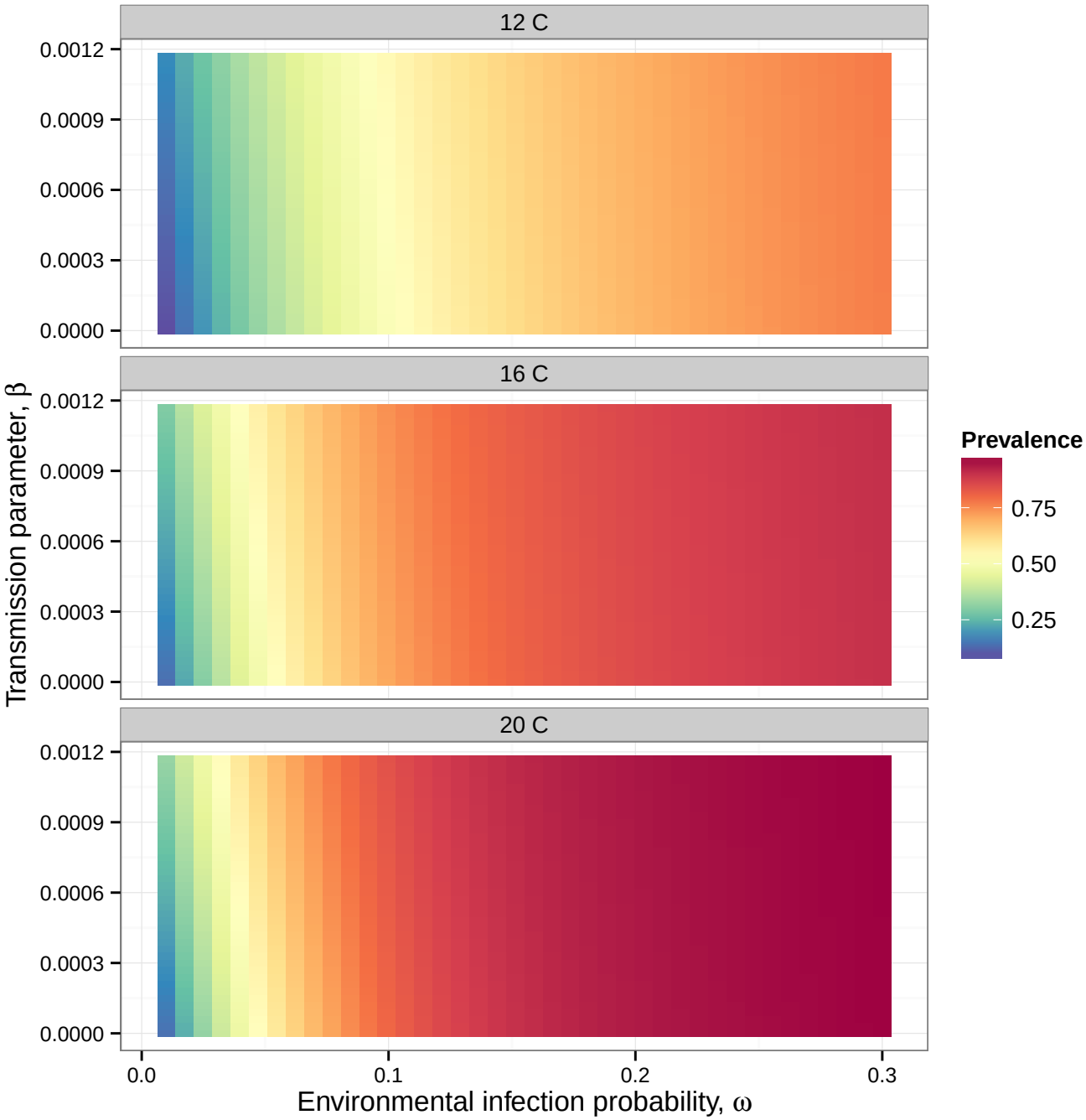

Figure 7: Prevalence of *Bd* at the end of a 120 day epizootic given different transmission coefficients (β) and environmental infection probabilities (ω) for the density-dependent transmission function. This plot shows 40 x 40 systematically chosen pairs of β and ω for which the *Bd*-prevalence dynamics were examined. Each panel shows the change in *Bd* prevalence in *Rana muscosa* populations with the different parameter combinations for a given temperature between 12 and 20 °C.

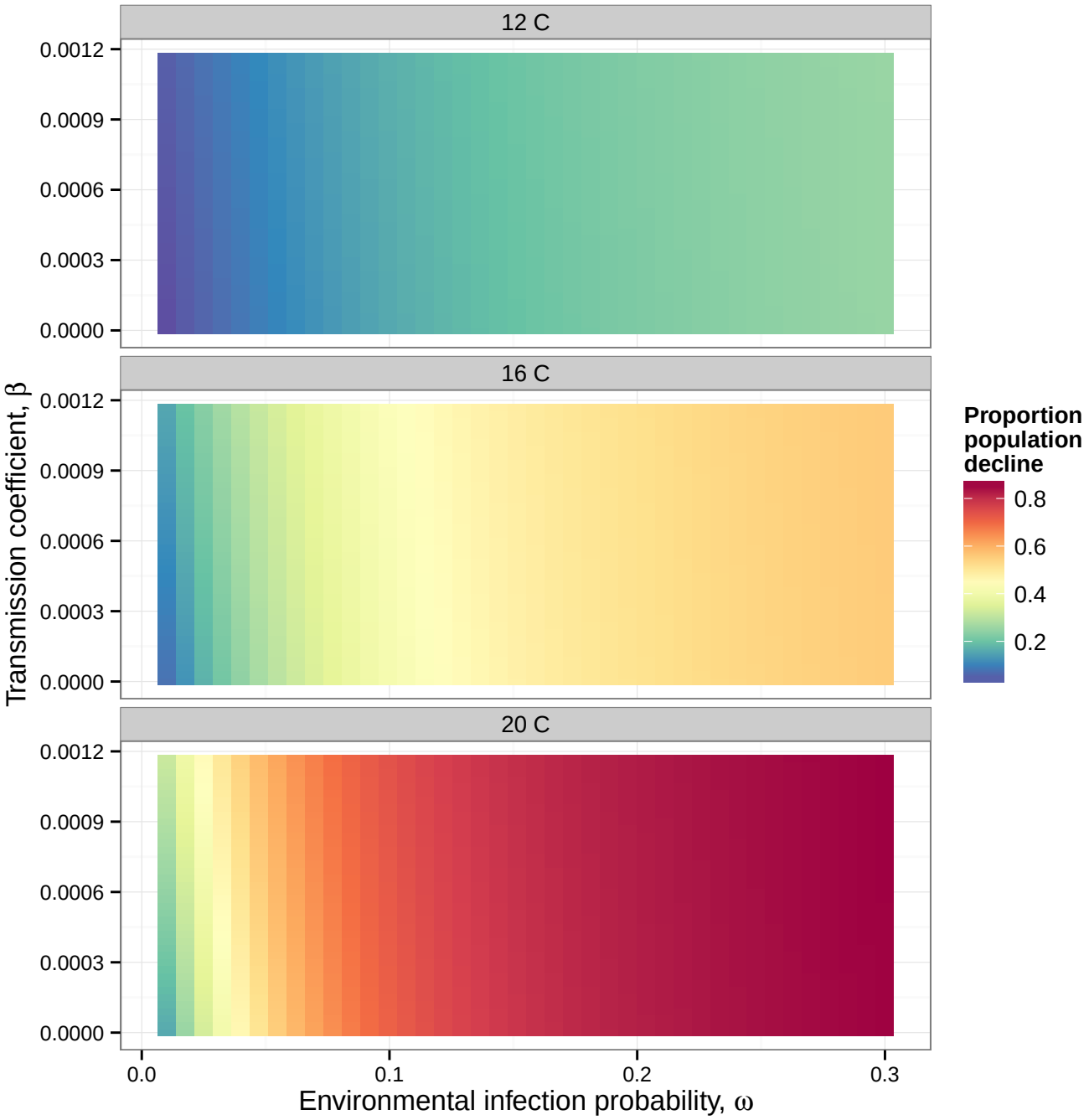

Figure 8: Proportional population loss of *Rana muscosa* at the end of a 120 day epizootic given different transmission coefficients (β) and environmental infection probabilities (ω) for the density-dependent transmission function. This plot shows 40 x 40 systematically chosen pairs of β and ω for which the population dynamics were examined. Each panel shows the change in proportional population loss for *R. muscosa* with the different parameter combinations for a given temperature between 12 and 20 °C.

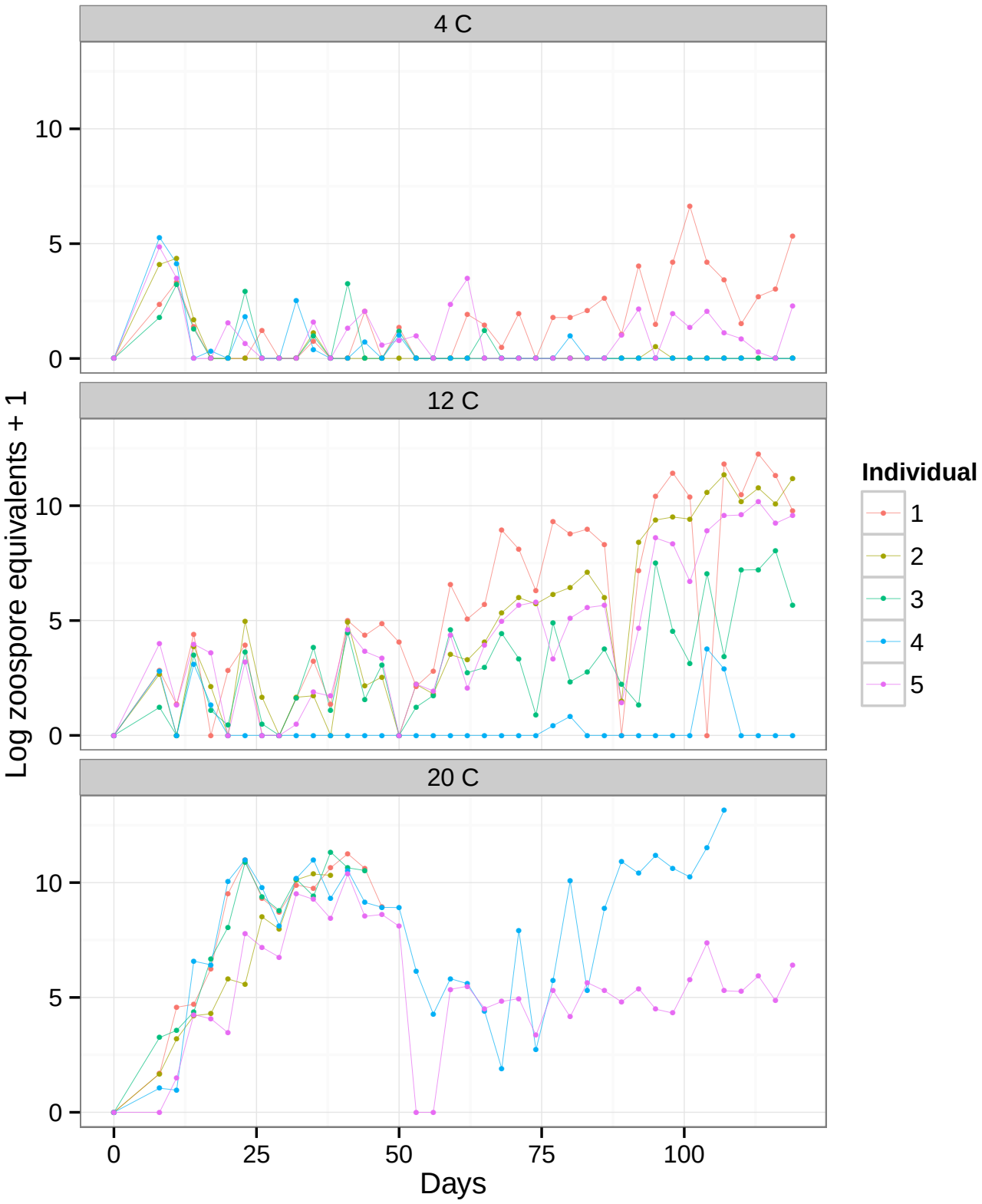

Figure 9: Infection trajectories of individual *Rana muscosa* housed at 4, 12, and 20 °C. Each line represents the *Bd* load trajectory of a particular *Rana muscosa* individual.

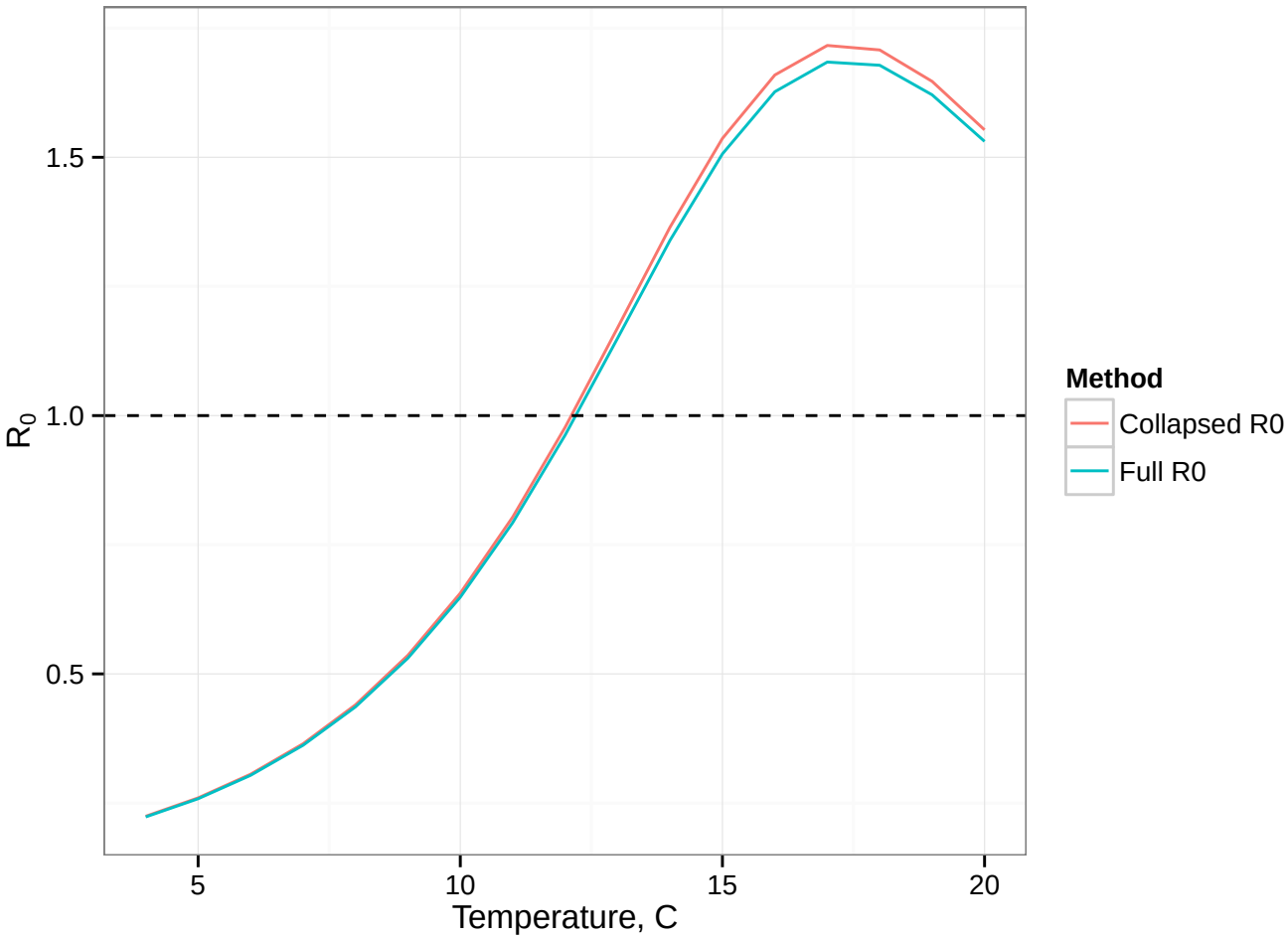

Figure 10: Plots of R_0 for a *Rana muscosa-Bd* IPM with density dependent transmission parameterized based on the parameters provided in Table 1 in the main text. The only parameter that was not from Table 1 was the transmission coefficient β which was set to be $9.82e10^{-4}$ based on Rachowicz & Briggs (2007). The number of susceptible individuals in the initial population was set to $S^* = 100$. R_0 was computed using both equation 9 (the blue line, Full R_0) and equation 11 (the red line, Collapsed R_0)